An Innovative Control Strategy of a Single Converter for Hybrid Fuel Cell/Supercapacitor Power Source

Toufik Azib, Olivier Bethoux, Ghislain Remy, Claude Marchand, Éric Berthelot

Accepted Manuscript

An Innovative Control Strategy of a Single Converter for Hybrid Fuel Cell/Supercapacitors Power Source

Toufik Azib, Olivier Bethoux, Ghislain Remy, Claude Marchand, Eric Berthelot

101 paper citations according to IEEE explore, on March 1, 2019

Document Version:	Early version, also known as pre-print

An Innovative Control Strategy of a Single Converter for Hybrid Fuel Cell/Supercapacitors Power Source

T. Azib, O. Bethoux, *Member, IEEE*, G. Remy, *Member, IEEE*,
C. Marchand *Member, IEEE*, and E. Berthelot,

Abstract—**In this paper, an innovative control strategy for hybrid power source dedicated to automotive applications is detailed. Firstly, an analysis of classical hybrid architectures using FC / SCs is presented. Then, an analysis of load requirements for automotive applications is proposed. A new control strategy of a single converter, based on cascaded control loop with a decoupling strategy in the frequency domain, is fully explained. Finally, experimental results on a Ballard PEMFC are presented to illustrate the effectiveness of the proposed method.**

Index Terms— **Supercapacitor, fuel cell, power electronics, efficiency and reliability enhancement, real-time control systems, transports applications.**

I. INTRODUCTION

THE use of hydrogen as an energy carrier is of increasing interest to individuals, companies and countries due to the range of its potential benefits [1]. Currently, fuel cells (FC) can be used in embedded systems such as electric vehicles [2] and can produce clean electricity directly; the only residue is water. However, this technology has some weak points, including final cost and mass production, reliability as well as durability [3]. Fuel cell performances (efficiency, degradation, aging effects) are influenced by many environmental and application constraints: electronic converters [4], environment temperature, the presence of water in the stack, gas polluting, vibrations, power demand, gas supply… [5], [6], [7].

Among those parameters, load current transients seem to be essential: short cycles (about 1 min) with high ratios of peak power to average power lead to an irreversible cell voltage decrease (0.1 V for a 0.68 V cell in 100 hours). Then, the cell voltage has a decay rate close to 80 μV.h^{-1}, whereas the same stack exhibits a constant voltage decay rate per cell of 50 μV.h^{-1} when mainly operating at peak power [8], [9].

These aging tests prove that limiting the load dynamic effects can save the FC performances and raise its durability.

Consequently, in many applications such as transportation,

fuel cells should not be used alone. Then, auxiliary sources provide the fast power demand, allow regenerative energy recovery [9]-[11], and palliate the PEMFC short failure. For fast power demands, storage devices as supercapacitors (SCs) seem to be the best suitable components [12]-[14].

The challenges of fuel cell hybridization are the following: reaching FC lifetime requirements and fulfilling load performance specifications without increasing the global cost. To reach these goals, better power sources architecture and proper related energy management controllers have to be designed.

Many hybrid fuel cell system configurations have been studied and documented [15]-[17]. They can be classified in three main categories [15], [16]: series, parallel and cascaded architectures. It has also been proven that the parallel structure is the most advantageous one [16], [17]. Many advantages can be stressed: less component constraints, simple energy management, and good reliability.

Many power electronics architectures have been associated to hybrid power sources [15]-[17], including: the two-converter structure, the direct structure and the one-converter structure. The two-converter structure consists in associating a static converter and a control loop to each power source (Fig. 1). It leads to a good control but has many more losses. The direct parallel structure consists in connecting the FC directly to the load without a power converter (Fig. 2). It induces a low cost but also has a low FC controllability.

Different control strategies have been described for hybrid system power management [18]-[30]. Most common strategies are based on voltage regulation of the DC bus [18], [19], [25]-[28], on the evolution of the state of the system [21 [22], on fuzzy and neural network controls [23], [24], [30] and on passivity and flat systems [20], [29].

In this paper, a structure of hybrid FC/SCs power source with a single power converter is proposed. A control strategy is developed for the energy management of the different sources supplying the load. The proposed strategy is based on the regulation of the DC bus voltage and uses the natural frequency decoupling of each source (DC bus capacitor, SCs and FC). An experimental study has been developed to validate the effectiveness of the architecture and the supervision strategies.

II. HYBRID POWER SYSTEM DESCRIPTION

A. Description of the Hybrid Power Structures

A hybrid power source is generally composed of different specific power sources, as FC and SCs, which enable the global system to provide the permanent and transient powers demanded by the load. Three hybrid power sources structures are mainly used:

- The two-converter structure consists in associating a static converter and a control loop to each power source, as shown in Fig. 1. This control strategy generates a large number of degrees of freedom in the control design [17]-[20]. However, its drawback lies in the inevitable losses associated with every static converter.
- The direct parallel structure consists in connecting the fuel cell directly to the load, as shown in Fig. 2. Its main drawback is related to over-sizing the SCs necessary to fulfill the FC power requirements [31].
- The one-converter structure consists in adjusting the power fluxes (Fig. 3). Its main advantages are simplicity and reduction of both losses and costs of the power management interfaces and a good controllability.
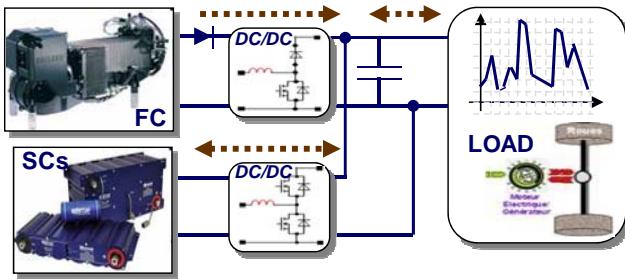

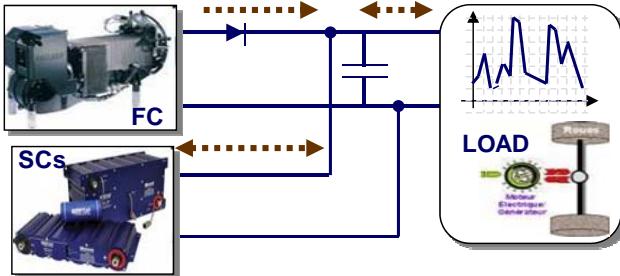Fig. 1. Two-converter parallel structure for FC/SCs hybrid power system.

Fig. 2. Direct parallel structure for FC/SCs hybrid power system.
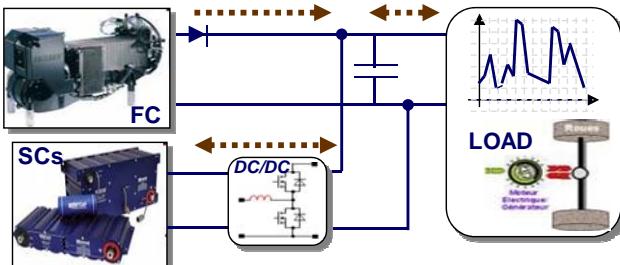

Fig. 3. One-converter parallel structure for FC/SCs hybrid power system.

These energy conversion architectures must be defined to allow a continuous functioning of the hybrid source with good performances and limited component deteriorations. Hence, the hybridization purpose is to:

- Comply with the low fuel cell dynamics;
- Recover the power generated by the load in generative mode and by the fuel cell during load power decrease.

Thus, the studied hybrid structure (Fig. 3) faces several modes of operation:

- Normal mode. The main source supplies the electric load and maintains the auxiliary source voltage.
- Discharge mode. Both energy sources supply the electric load simultaneously.
- Recovery mode. The electric load supplies the storage devices. The supercapacitor level of charge increases while the FC power drops slowly. If the SCs are completely charged, then, exceptionally, the extra energy will be transferred into a dissipative safety device.

B. Description of the Hybrid Structure Model

The FC static behavior is only considered because the fuel cell is controlled with slow dynamics. With this assumption, the FC voltage V_{FC} becomes lower than the open circuit voltage E_{FC} as the FC current i_{FC} increases because of the three main irreversible losses [32]:

$$V_{FC} = E_{FC} - Ri_{FC} - A\ln(i_{FC} + i_l) - m\exp(ni_{FC}) \qquad (1)$$

Where R is the membrane resistance; A is the Tafel coefficient; and m and n are coefficients of the mass transfer equation [32].

Hence, the fuel cell characteristic can be considered as a voltage source with ohmic, kinetic and mass transfer resistances [32]. Consequently, the fuel cell can be connected in parallel to the DC bus, which is a perfect voltage source with its associated capacitor C_{BUS}. The capacitor value has to be small in order to prevent difficult starting procedures. Indeed, with a large capacitor value (from associating SCs and FC in parallel, as shown in Fig. 2), the FC power would be synchronized with the SCs state of charge. Important FC power demands imply low FC supply voltage, which induces low SCs state of charge and *vice versa*. Hence, to simplify the starting procedure and to face any load profiles without over-sizing the auxiliary storage devices (SCs), it is relevant to connect SCs and FC with a chopper (Fig. 3). SCs state of charge and FC power are then decoupled and the single buck-boost converter only operates discontinuously, since it adapts voltage and current values to the transient auxiliary source.

As a consequence, a supervision device must be designed in order to monitor this converter. It needs to ensure the continuity of operation from the user's point of view and guarantee an adapted use of each source. This paper's aim is to show that, in spite of a simplified architecture and a reduction of the degrees of freedom, the power management remains simple and effective.

III. LOAD REQUIREMENTS STUDY

As mentioned before, fuel cell systems are significantly affected by aging effects due to high load current dynamics. This fact limits FC use to some niche markets. However, many other applications can be achieved by FC with an associated impulse power device. For instance, the electrical vehicle application illustrates the need for FC hybridization well. Hence, this architecture and its associated control structure are implemented for a load profile close to car requirements.

The needed car power is mainly due to speed variations, tire friction dissipation, aerodynamics dissipation and mass elevation. This power, P_{motor}, can be expressed as:

$$P_{motor} = V\left(C_r Mg\cos(\alpha) + Mg\sin(\alpha) + M\frac{dV}{dt} + \frac{1}{2}\rho SC_x V^2 \right) \quad (2)$$

Where:
V and M are the vehicle speed and mass (in m.s^{-1} and kg);
α is the road angle with an horizontal line (in rad);
C_r and C_x are the friction and aerodynamic coefficients;
ρ is the air density (in kg.m^{-3});
S is the front surface area (in m^2).
M=1000; g=9,81; α=0; Cr=0,01; Cx=0,30; ρ=1,225; S=2,5.

The vehicle power demand can hence be determined by the driver's requirements. For testing vehicles, driving cycles have been normalized. European light duty vehicles have to face the New European Driving Cycle (NEDC) which represents the typical usage of a car in Europe. The NEDC consists of repeated urban cycles (called ECE-15 driving cycle) and an Extra-Urban driving cycle, or EUDC. Fig. 4 shows the ECE-15 cycle with the speed and the power demand of a car following a flat road. Sudden power changes can be noticed each time the driver requires a speed change. In this example, the car's average power is only of 0.72 kW, whereas the peak power reaches roughly 10 kW, which means a 13.7 ($P_{max}/P_{average}$) ratio.

For those reasons, the proposed control strategy is evaluated with a severe profile consisting of raising and falling power edges.

Fig. 4. ECE-15 Driving Cycle.

IV. CONTROL STRATEGY OF THE HYBRID POWER SYSTEM

The proposed control strategy is based on a power decoupling strategy in the frequency domain of the power source. This energy-management strategy fulfills the fast energy demands of the load and respects the integrity of each source. Precisely, the main idea is to assign the load power demands to the appropriate source, as shown in Fig. 5:

Fig. 5. Bandwidth splitting technique

A. Description of the Control Structure

This frequency decoupling technique leads naturally to a cascaded control loop, as depicted in Fig. 6, with:
- A current closed loop controlling the SCs current;
- A voltage closed loop controlling the DC Bus voltage;
- A compensation closed loop controlling the SCs State of Charge (SOC).

Fig. 6. Control strategy block diagram

To limit the fuel cell dynamics, the DC bus voltage value has to evolve in a slow controlled way. Thus, the FC supplies the low frequency (LF) of the current load demands, as depicted in Fig. 5. Then, the SCs deal with the medium frequency (MF) load range. Because the SCs have a large capacity compared to the DC bus, they regulate the DC bus voltage. Besides, the bus capacitor C_{BUS} is designed regarding the high frequency (HF) of the current load requirements. Finally, the cascaded control loops drive the duty cycle of the DC chopper PWM.

B. DC Chopper Model

The buck-boost chopper (Fig. 7) is modeled according to its average behavior and can be analyzed with the following set of equations:

$$C_{BUS} \cdot \frac{dV_{BUS}}{dt} = (i_{SC})' + i_{FC} - i_{LOAD} \tag{3}$$

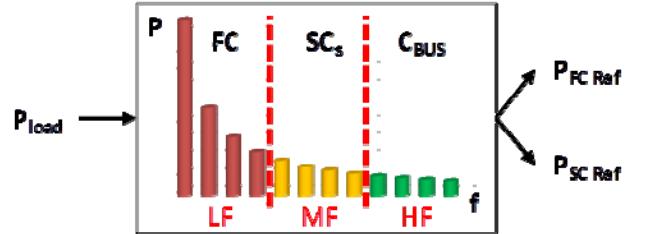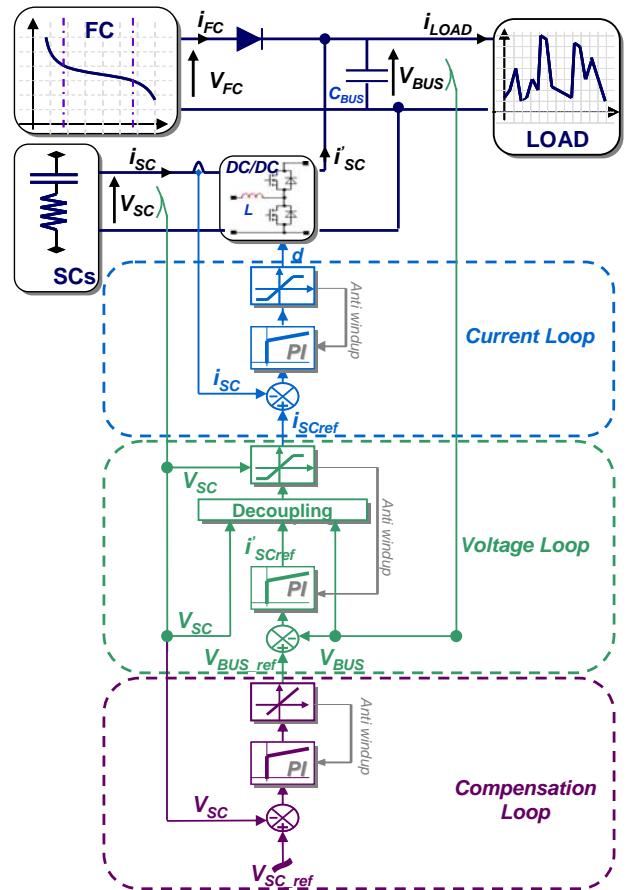$$C_{SC} \cdot \frac{dV_{SC}}{dt} = -i_{SC} \tag{4}$$

$$L \cdot \frac{di_{SC}}{dt} = V_{SC} - d \cdot V_{BUS} \tag{5}$$

Where:
- L has a small value, as the inductor function is to filter the switching frequency;
- C_{BUS} value is determined to filter the switching frequency and the high load power frequency range;
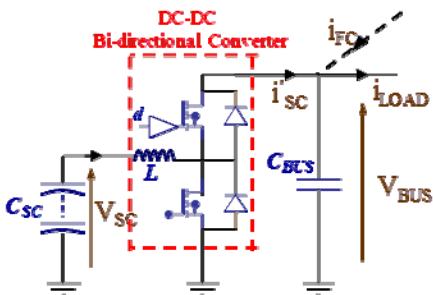- *d* is the PWM duty cycle of the chopper and acts as the unique control value of the whole power system.

Fig. 7. Architecture of DC-DC Converter

C. Control Strategy Design

In the following section, the design of the control strategy (Fig. 6) is described more thoroughly.

1) Current Loop: The inner control loop is tuned to drive the SC current. As $V_{BUS}(t)$ is time dependant, (5) is a non-linear first order equation. Nevertheless, the bus capacitor value C_{BUS} is designed to filter higher frequencies than the cut-off frequency of the current loop. With this assumption, $V_{BUS}(t)$ can be considered constant during $i_{SC}(t)$ regulation. Hence, using the Laplace transform, (5) becomes:

$$i_{SC}(s) = \left[-\frac{V_{BUS}}{Ls} \right] d(s) + \left[\frac{1}{Ls} \right] V_{SC}(s) \tag{6}$$

Where V_{SC} acts as a low frequency perturbation.

Hence, to reject this perturbation, a classical PI controller is proposed (Fig. 8).
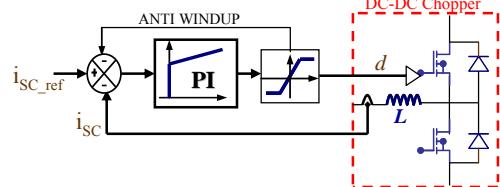
Fig. 8. Inner control loop insuring fast dynamics of SCs current

Then, the closed-loop transfer function of the system can be deduced:

$$H_{BF}(s) = \frac{\frac{V_{BUS}}{Ls} \frac{K_{P1}s + \omega_{I1}}{s}}{s + \frac{V_{BUS}}{Ls} \frac{K_{P1}s + \omega_{I1}}{s}} = \frac{1 + \tau_1 s}{1 + 2m_1 \frac{s}{\omega_{BF1}} + \left(\frac{s}{\omega_{BF1}} \right)^2} \tag{7}$$

Where, ω_{BF1} is the natural frequency of the closed loop; m_1 is the damping ratio; τ_1 is the time constant of its zero; K_{p1} is the proportional gain of the regulator, and ω_{I1} is the integral gain of the regulator.

$$\omega_{BF1} = \sqrt{\frac{V_{BUS}}{L} \omega_{I1}}, \quad m_1 = \frac{K_{P1}\sqrt{\frac{V_{BUS}}{L}}}{2\sqrt{\omega_{I1}}} \quad \text{and} \quad \tau_1 = \frac{K_{P1}}{\omega_{I1}} \tag{8}$$

The current loop dynamics is tuned to get a closed loop time response of about five to ten times the switching periods and the desired damping ratio is settled to $m_1 = 1$. So, the PI corrector parameters are given:

$$\omega_{I1} = \frac{(\omega_{BF1})^2}{A_1}, \quad K_{P1} = \frac{2m_1 \cdot \omega_{BF1}}{A_1} \quad \text{and} \quad A_1 = \frac{V_{BUS}}{L} \tag{9}$$

With $V_{BUS} = 48$ V, $L = 50$ µH, and $f_{BF1} = 1$ kHz, then:

$$\omega_{I1} = 39,5\ rad.s^{-1} \quad \text{and} \quad K_{P1} = 0,0126 \tag{10}$$

An anti-windup compensator is added to take into account the duty cycle range $(0 < d < 1)$ (Fig. 8). This anti-windup compensator only acts in the case of control value saturation. It maintains the closed loop system in a linear domain.

Moreover, to prevent current overshoot, the zero of the closed loop should be compensated by a low pass filter, with a time constant of about:

$$\tau_1 = \frac{K_{P1}}{\omega_{I1}} = \frac{0,0126}{39,5} \approx 0,32\ ms \tag{11}$$

The current loop reference is given by the slower voltage loop detailed in the following paragraph. Indeed, the voltage loop ensures that the DC bus is accurately controlled.

2) Voltage Loop: This strategy ensures the rejection of the load perturbations on the bus voltage, which remains unaffected by any breaking SCs over-current. As far as the

imbricated loops assume a frequency decoupling, the control strategy remains efficient. Precisely, it means the voltage loop time response has to be ten times slower than the current loop time response.

The second cascaded loop has to monitor the bus voltage $V_{BUS}(t)$: the faster this voltage tracking, the smaller the C_{BUS} value. A PI controller is designed following a similar strategy to the current loop. This control is possible because the average current $i_{SC}'(t)$ provided by the chopper to the DC bus is linked to the supercapacitor current $i_{SC}(t)$. Considering no chopper losses and the fact that the inductor is a small storage device compared to the C_{BUS} capacitor, then:

$$v_{SC} \cdot i_{SC} = V_{BUS} \left(i_{SC} \right)' \tag{12}$$

Considering (7), (12) becomes:

$$C_{BUS} \cdot \frac{dV_{BUS}}{dt} = \left[\frac{V_{SC}}{V_{BUS}} \right] i_{SC} + i_{FC} - i_{LOAD} \tag{13}$$

(13) is a nonlinear first order equation, but both $V_{BUS}(t)$ and $V_{SC}(t)$ are measured variables. Hence (13) can be linearized by replacing the actual control variable (i_{SC_ref}) by a virtual variable (i_{SC_ref})' with the decoupling equation (14).

$$i_{SC\_ref} = \left[\frac{V_{BUS}}{V_{SC}} \right] \left(i_{SC\_ref} \right)' \tag{14}$$

From (13) and (14), the following expression is useful to design the output voltage control loop:

$$V_{BUS} = \frac{\left(I_{SC\_ref} \right)}{C_{BUS} s} + \frac{I_{FC}}{C_{BUS} s} - \frac{I_{Load}}{C_{BUS} s} \tag{15}$$

So the output of the second regulator can be (i_{SC_ref})' and i_{SC_ref} is computed with the decoupling function (14). Figure 9 illustrates this principle.
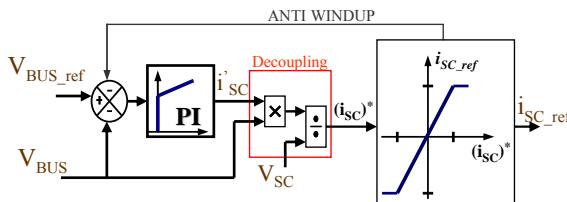

Fig. 9. Voltage control loop scheme insuring load perturbation rejection

Then, the closed-loop transfer function of the system can be deduced as a second order transfer function, where:

$$\omega_{BF2} = \sqrt{\frac{\omega_{I2}}{C_{BUS}}}, \ m_2 = \frac{K_{P2}}{2\sqrt{\omega_{I2} C_{BUS}}} \text{ and } \tau_2 = \frac{K_{P2}}{\omega_{I2}} \tag{16}$$

To respect dynamics decoupling, the voltage loop must present a time response ten times higher than the current loop, and the desired damping ratio is settled to $m_2=1$. So, the PI corrector parameters are given:

$$\omega_{I2} = C_{BUS} \left(\omega_{BF2} \right)^2 \text{ and } K_{P2} = 2m_2 \cdot C_{BUS} \cdot \omega_{BF2} \tag{17}$$

With, $C_{BUS} = 10 \text{ mF}$ and $f_{BF2} = 100 \text{ Hz}$, then:

$$\omega_{I2} = 39{,}5 \ 10^3 \ rad.s^{-1}, \ K_{P2} = 12{,}6 \text{ and } \tau_2 \approx 0{,}32 \ ms \tag{18}$$

A current saturation and an anti-windup compensator are used to limit the $i_{SC\_ref}(t)$ control range and protect the SCs:

$$i_{SCmin} \left(t \right) < i_{SCref} \left(t \right) < i_{SCmax} \left(t \right) \tag{19}$$

Those feedback loops allow us to hold the FC operating point, whatever the load power demand. It implies a change in the SCs' state of charge. For this purpose, a compensation loop has been implemented.

3) Compensation Loop: At that point, the two cascaded control loops allow driving the DC bus voltage precisely while taking the SC requirements into account. As SCs erase the V_{BUS} voltage ripple due to some transient load power demands, the state of charge of the SC evolves. With $V_{BUS}(t)$ tracking, the system is able to manage the FC operating point, which is the compensation loop purpose. Referring to (1), the relation between $V_{BUS}(t)$ and $i_{FC}(t)$ is nonlinear. Hence, the compensation loop is designed using a small-signal model approach. Around a fuel cell operating point, (1) is linearized showing FC current variation δi_{FC} versus BUS voltage δv_{BUS} :

$$\delta I_{FC} = -G \delta V_{BUS} \tag{20}$$

With a positive parameter ranging from G_{min} to G_{max}.

Referring to (4) and (9), the SC voltage variation δv_{SC} induced by FC current variation δi_{FC} can be computed through ($\delta i'_{FC}$) knowledge. This latter small-signal variable can be deduced from the voltage loop regulator and the fuel cell behaviour:

$$\delta I'_{SC} \left(s \right) = \frac{K_{P2} s + \omega_{I2}}{s} \times \left[\delta V_{BUSref} \left(s \right) - H_1 \left(s \right) \times \right. \\ \left. \left[-\delta I_{load} \left(s \right) - G \delta V_{BUSref} \left(s \right) + \delta I'_{SC} \left(s \right) \right] \right] \tag{21}$$

Considering (4), (14) and (21), the link between BUS voltage variations and the SC voltage variations can be exhibited in (22):

$$\delta V'_{SC} \left(s \right) = H_{3BUS} \left(s \right) \times \delta V_{BUSref} \left(s \right) + H_{3load} \left(s \right) \times \delta I_{load} \left(s \right) \tag{22}$$

Here:

$$H_{3BUS} \left(s \right) = -\frac{V_{BUS} \cdot G}{V_{SC} \cdot C_{SC} \cdot s} \times \frac{\left(1 + \tau_3 s \right)}{1 + 2m_2 \dfrac{s}{\omega_{BF2}} + \left(\dfrac{s}{\omega_{BF2}} \right)^2} \tag{23}$$

$$\tau_3 = \frac{C_{BUS}}{G} \tag{24}$$

With the system parameters this transfer function H_{3BUS} exhibits an integrator associated with a second order filter having zero and poles in much higher frequency than the

compensation loop bandwidth specification. Indeed, the desired bandwidth is less than 1 Hz. Thus, after decoupling, the third PI controller is tuned using an integrator with a bounded gain.

$$H_{3BUS}(s) \cong -\frac{G}{C_{SC}s}$$ (25)

With $G_{max} = 1$ S, $C_{SC} = 125$ µF, and $f_{BF2} = 1$ kHz, then:

$$\omega_{I3} = 0,58 \ rad.s^{-1} \text{ and } K_{P3} = 9,3$$ (26)

As far as the anti-windup compensator is taken into account, we must underline that to limit the slope rate of the fuel cell current, the slope rate of the DC bus voltage is limited. Figure 10 illustrates this principle:
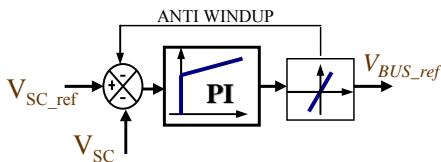

Fig. 10. Compensation loop scheme with a SC state of charge regulation

The reference value V_{SC_ref} is constant and determined so as the amount of energy the SC can collect $+\Delta E_{SC}$ is equal to the one it can restore $-\Delta E_{SC}$.

4) Conclusion: This cascaded control structure shows that, even though the one-converter parallel structure is a very simple architecture with a single degree of freedom, and could satisfy the different requirements of the hybrid system both from the point of view of the feed load and from the point of view of the components limits.

V. EXPERIMENTAL RESULTS

As shown in Fig. 3 and Fig. 6, the one-converter architecture and its associated control strategy have been tested both in simulation and using a 1 kW experimental set-up. This section presents the test bench specifications and the experimental results.

A. Test Bench description

Fig. 11 presents the experimental test bench.

The Nexa fuel cell designed by Ballard has been chosen. Indeed, many fuel cells technologies are under development. Among them, the Proton Exchange Membrane Fuel Cell (PEMFC) is the most likely candidate for transport applications. A quick start-up and high power densities are some key advantages that make PEMs a promising technology for the automotive market [32]. This Nexa fuel cell generator is composed of 46 cells and has a nominal power of 1200 W.

The transient auxiliary source consists of two Maxwell SC modules associated in series: each module is achieved with the connection of six individual elements in series [2.7 V, 1500 F]. This SCs device is interconnected to the DC bus using a chopper built with standard IGBT modules (SEMITRANS: SKM50GB123D). The switching frequency of the PWM is set

to 25 kHz. The buck-boost inductor has a value of 100 µH with a rated current of 150 A. The DC bus capacitor has a 10 mF value.

A real-time dSPACE DS1104 controller board has been used for implementing the energy management control strategy, using Matlab/Simulink software.

The cascaded control loops, which generate the duty cycle reference d, have been implemented with digital PI controllers. Measurements are performed in the dSPACE controller board through A/D converters working at a 25 kHz sampling frequency.

The hybrid power source is connected to a programmable electronic load (Höcherl & Hackl, model ZS1806), which has a rated power of 1800 W (i_{max} =150A / V_{max} = 60V). This load emulates vehicle power consumption, and is directly monitored by the dSPACE real-time card.

Table 1 shows the electric characteristics of the on-board power sources.

B. Analysis of results

Experiments have been performed on the experimental set-up to validate the previously explained control strategies:
- The three cascaded closed-loops are properly decoupled.
- The compensation loop efficiently ensures the required FC dynamic, regarding the FC static voltage/current characteristic. For that purpose, the time response of the hybrid system is analyzed.

The first load cycle shows fast transient reactions as well as some steady state behaviors. It consists in a square waveform of the power demand characterized by a 5 mHz frequency, a 50 W low level, and a 400 W high level. The main variable waveforms of the hybrid system are depicted in Fig. 12. The first subplot (Fig. 12a) shows that the required load power is

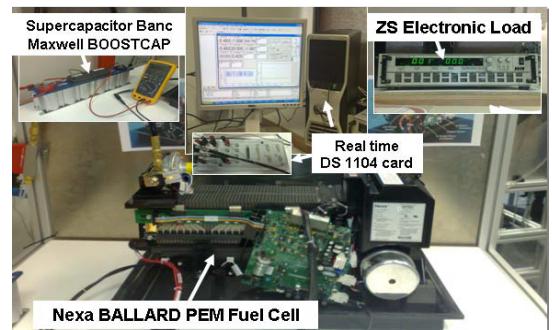Fig. 11. Experimental bench components

TABLE I
ELECTRIC CHARACTERISTICS OF POWER SOURCES

Fuel Cell: Parameter Name	Value
Open Circuit Voltage	45 V
Rated Voltage	26 V
Rated Current	46 A
Supercapacitor: Parameter Name	Value
Capacitance	125 F
Rated Voltage	32 V
Rated Current	200 A

supplied by two complementary sources. The SCs auxiliary source reacts immediately after each load power edge and behaves as a high-band pass filter with a time response of a few milliseconds. Besides, the FC slowly reacts to the load changes and responds as a low-band pass filter with a time response of a few seconds. Figure 12b presents each source current and shows that the control loops force each source to respect its own characteristics. Main source current i_{FC} smoothly increases from 1 A to 15 A with a 1.5 A.s^{-1} slope. Furthermore, the SCs state of charge is well managed since, in steady state, SCs voltage tends to its reference value (24 V) (Fig. 12c). SCs temporary assist the FC and imply a SCs voltage change. But in the meantime, the slow FC reaction ensures a good regulation of the SCs voltage. Indeed, this explains the small overshoot of FC power during the transient SCs voltage compensation (Fig. 12a and 12d). The FC voltage (Fig. 12d) varies inversely to the FC current. It is relevant with the static FC model composed of an electromotive force and a resistance in series.

The second experiment is carried out to validate the proposed management strategy on a power cycle representative of a vehicle power demand (Fig. 13). The load requirement consists in raising and falling power edges between 0 W and 800 W. Note on SCs current ($i_{SC}(t)$) that the compensation action is very effective even though the very fast dynamic of power demand (Fig. 13). Therefore, each load change doesn't affect the FC current and voltage ($i_{FC}(t)$, $V_{FC}(t)$) instantaneously (Fig. 13b, Fig. 13d). Nevertheless, the FC tends to set the SCs to its nominal SOC. So, the SC voltage fluctuates around its constant reference value V_{SCref} (24 V)
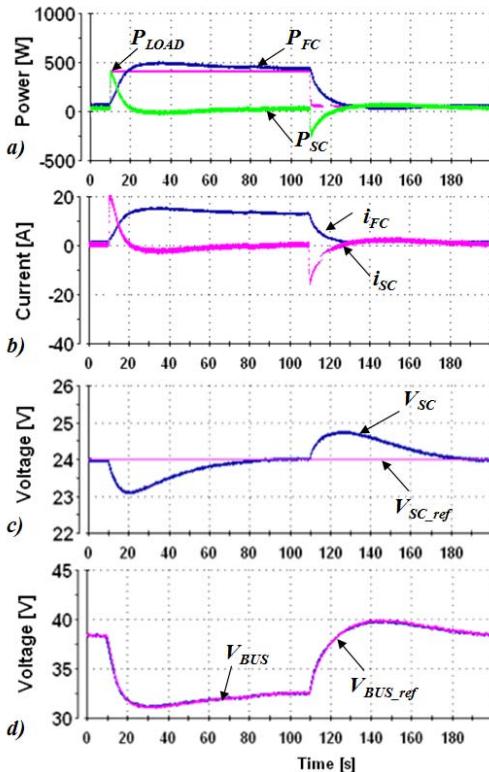
continuously, as shown in Fig. 13c. Notice at each power load decrease, SCs current sign changes in order to absorb over energy from the DC bus produced by fuel cell and inducing the increase of the SCs SOC.

The anti-windup compensation of each loop acts briefly. It avoids PI controller overshoot. Thus, each control loop is never subjected to any time delay. Hence, anti-windup compensation enables each control loop to remain close to a linear mode. For instance, Fig. 14 depicts voltage loop compensation action during a complete cycle.

The experiment results reveal and confirm the efficiency of the control strategy of the one-converter structure. In particular, it can be observed the following keypoints:
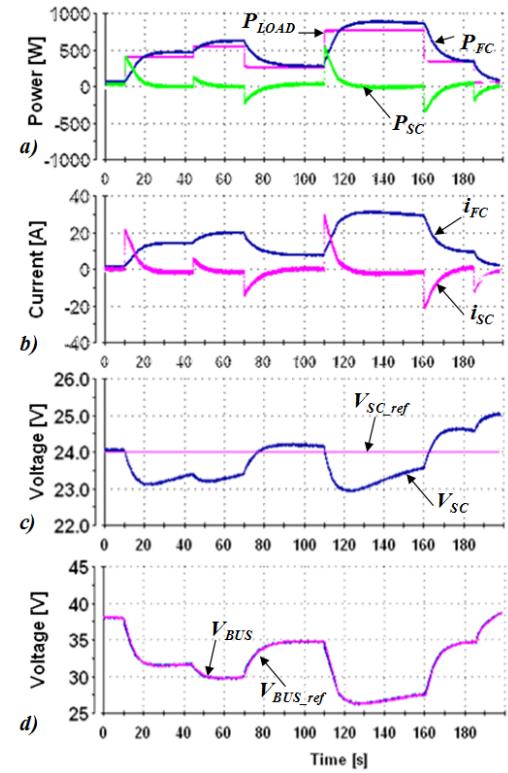- The SCs supply most of the transient power required by load.

Fig. 13. A complete hybrid system response on a load cycle.

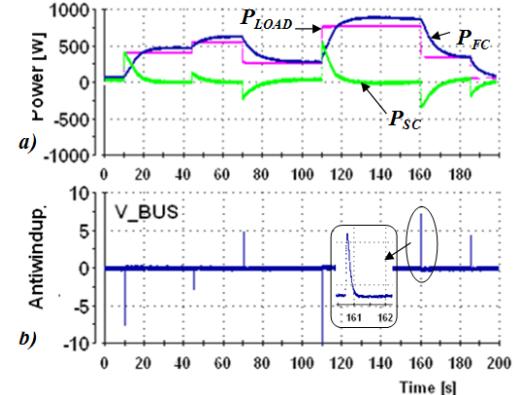Fig. 12. A low frequency square power demand.

Fig. 14. Anti-windup output waveform of the voltage loop.

- The SCs power has the fastest dynamics; the FC power has the slowest dynamics and both are well tuned.
- The load requirements are always satisfied on the whole driving cycle

VI. CONCLUSION

This paper deals with the electrical power hybridization of a PEMFC, which has already been proved to be relevant for FC lifetime enhancement [29]. A FC/SCs hybrid architecture has been proposed to minimize the number of power static converters. It uses a single power converter dedicated to the transient source (SCs). A complete control structure has been developed and successfully implemented. It has been shown that the hybrid source is able to provide any load demand and to satisfy the sources' inherent characteristics: FC and SCs voltage and current limits are considered, as well as slow FC dynamics. Despite its single degree of freedom, this innovative control strategy has been proved to be simple and effective.

The studied hybrid system can be easily adapted to different FC and SCs specification requirements and can be scaled to many applications.

REFERENCES

[1] OECD Publishing, "Energy Technology Analysis, Prospects for hydrogen and Fuel Cells", *International Energy Agency*, Dec. 2005.

[2] Z. Jianli, C. Chakrabarti, L. Kyungsoo , C. Naehyuck S. Vrudhula, "Maximizing the Lifetime of Embedded Systems Powered by Fuel Cell-Battery Hybrids", Very Large Scale Integration (VLSI) Systems, IEEE Transactions on, Vol.17, No.1, Jan. 2009, pp.22-32.

[3] C. Borroni-Bird, *MacMillan Encyclopedia of Energy*, Ed. New York: MacMillan, 2000, Ch. Fuel Cell Vehicles.

[4] B. Wahdame, L. Girardot, D. Hissel, F. Harel F. Harel, X. François, D. Candusso, M. C. Péra1, and L. Dumercy "Impact of power converter current ripple on the durability of a fuel cell stack", *Int. Symposium on Industrial Electronics, IEEE-ISIE08*, July. 2008, pp.1495–1500.

[5] F. Harel, X. François, D. Candusso, M-C. Péra, D. Hissel, and J-M. Kauffmann, "PEMFC durability test under specific dynamical current solicitation linked to vehicle road cycle", *Fuel Cells from Fundamentals to Systems, Wiley-VCH*, Vol. 7, Issue 2, April 2007, pp 142-152.

[6] B. Wahdame, D. Candusso, X. François, F. Harel, M.C. Péra, D. Hissel, and J.-M. Kauffmann, "Comparison between two PEM fuel cell durability tests performed at constant current under solicitations linked to transport mission profile," *Int. Journal of Hydrogen Energy*, Vol.33, No.14, Jul. 2008, pp.3829-3836.

[7] Mestan Tekin, Daniel Hissel, Marie-Cécile Pera, Jean Marie Kauffmann, "Energy-Management Strategy for Embedded Fuel-Cell Systems Using Fuzzy Logic," *IEEE Trans. on Industrial Electronics,* vol. 54, no. 1, pp. 595-603, Feb 2007.

[8] N. Guillet, *et al.*, "Scientific and Technological Progress Toward the Development of an 80kWe PEM Fuel Cell System for Transport Applications", *Symposium. EVS-23*, Anaheim USA, Dec. 2007.

[9] P. Corbo, F. Migliardini, and O. Veneri, "Dynamic behaviour of hydrogen fuel cells for automotive application," *Elsevier,* Renewable Energy, Vol.34, No.8, Aug. 2009, pp.1955-1961.

[10] G. Hoogers, *Fuel Cell Technology Handbook*, CRC Press, Ch10, Oct. 2002, ISBN: 0768007062.

[11] Haimin Tao, J.L. Duarte, M.A.M. Hendrix, "Line-Interactive UPS Using a Fuel Cell as the Primary Source," *IEEE Trans. on Industrial Electronics,* vol. 55, no. 8, pp. 3012-3021, August 2008.

[12] B. Destraz, P. Barrade, and A. Rufer, "Power Assistance for Diesel – Electric Locomotives with Supercapacitive Energy Storage", *Power Electronics Specialists Conference*, IEEE-PESC'04, 2004.

[13] A. Schneuwly, M. Bärtschi, V. Hermann, G. Sartorelli, R. Gallay, and R. Kötz, "BOOSTCAP Double-Layer Capacitors for Peak Power Automotive Applications", *Proc. of the 2nd Int. Advanced Automotive Battery Conference*, AABC, Feb. 2002.

[14] R. Kötz, S. Müller, M. Bärtschi, B. Schnyder, P. Dietrich, F. N. Büchi, and A. Tsukada, "Supercapacitors for Peak-Power Demand in Fuel-Cell-Driven Cars", The Electrochemical Society, Pennington, NJ, ECS Proceedings, Vol.4, 2001, pp. 564.

[15] F. Giulii, Capponi, M. Cacciato, "Using Super Capacitors in combination with Bi-Directional DC/DC Converters for Active Load Management in Residential Fuel Cell Applications", *1st European Symposium on Supercapacitors*, IEEE-ESSCAP'04, 2004.

[16] M. Cacciato, F. Caricchi, F. Giuhlii, and E. Santini, "A critical evaluation and design of bi-directional DC/DC converters for supercapacitors interfacing in fuel cell applications", *in Proc. Industry Applications Conf.*, IEEE IAS 2004, Oct. 2004, Vol.2, pp. 1127-1133.

[17] Z. Jiang, L. Gao, M.J. Blackwelder, and R.A. Dougal, "Design and experimental tests of control strategies for active hybrid fuel cell/battery power sources", *J. Power Sources*, Vol.130, 2004, pp. 163-171.

[18] P. Thounthong, S. Raël, and B. Davat, "Control strategy of fuel cell and supercapacitors association for distributed generation system", *IEEE Transactions on Industrial Electronics*, Vol. 54, No. 6, Dec. 2008.

[19] H. Tao, J. L. Duarte, and M. A. M. Hendrix, "Line-Interactive UPS Using a Fuel Cell as the Primary Source", *IEEE Transactions on Industrial Electronics*, Vol. 55, No. 8, Aug. 2008.

[20] Becherif, M Y Ayad, and A Miraoui, "Modeling and Passivity-based Control of Hybrid Sources: Fuel Cells and Super-Capacitors", *Industry Applications Conference*, IEEE-IAS'06, 2006, pp.1134 – 1139.

[21] K. Jin, X. Ruan, M. Yang, M. Xu, "A Hybrid Fuel Cell Power System," IEEE Trans. on Industrial Electronics, vol. 56, no. 4, pp. 1212-1222, April 2009.

[22] Z. Jiang, and R.A. Dougal, "A Compact Digitally Controlled Fuel Cell/Battery Hybrid Power Source", *IEEE Transactions on Industrial Electronics*, Vol.53, 2006, pp. 1094-1104.

[23] A. Hajizadeh, and M. A. Golkar, "Intelligent power management strategy of hybrid distributed generation system", *Elsevier*, Electrical Power and Energy System, 2007, pp.783–795.

[24] J. Moreno, M. E. Ortúzar, and J. W. Dixon, "Energy-Management System for a Hybrid Electric Vehicle, Using Ultracapacitors and Neural Networks," *IEEE Transactions on Industrial Electronics*, Vol. 53, No. 2, Apr. 2006, pp.614-623.

[25] J.N. Marie-Francoise, H. Gualous, R. Outbib, and A. Berthon, "42V Power Net with supercapacitor and battery for automotive applications", *Elsevier*, Journal of Power Sources, Vol.143, 2005, pp.275–283.

[26] P. Thounthong, S. Raël, and B. Davat, "Energy management of fuel cell/battery/supercapacitor hybrid power source for vehicle applications", *Journal of Power Sources*, Vol.193, No.1, Aug. 2009, pp.376-385.

[27] T. Azib, O. Bethoux, G. Remy, C. Marchand, "Structure and Control Strategy for a Parallel Hybrid Fuel Cell/Supercapacitors Power Source", *The 5th IEEE Vehicle Power and Propulsion Conference* (VPPC'09) Sept. 2009, Dearborn, MI, 2009.

[28] C. A. Ramos-Paja, C. Bordons, A. Romero, R. Giral, and L. Martínez-Salamero, "Minimum Fuel Consumption Strategy for PEM Fuel Cells, "IEEE Transactions on Industrial Electronics, Vol. 56, NO. 3, March 2009.

[29] A. Payman, S. Pierfederici, and F. Meibody-Tabar, "Implementation of a Flatness Based Control for a Fuel Cell-Ultracapacitor Hybrid System", *Power Electronics Specialists Conference*, IEEE-PESC'07, June 2007.

[30] M. Ortuzar, J. Moreno, J. Dixon, "Ultracapacitor-Based Auxiliary Energy System for an Electric Vehicle: Implementation and Evaluation," *IEEE Trans. on Industrial Electronics,* vol. 54, no. 4, pp. 2147-2156, August 2007.

[31] M Garcia Arregui, "Theoretical study of a power generation unit based on the hybridization of a fuel cell stack and ultracapacitors", Ph.D. dissertation, Dec. 4th 2007, Toulouse, France.

[32] F. Barbir, *PEM Fuel Cells*, New York: Elsevier Academic Press, 2005.

Toufik Azib was born in Bougaa, Algeria, in 1983. He received the Electrotechnical Engineering Diploma

from the University of Setif, Algeria in 2006. He also received the M. Sc. degree in Electrical Engineering from Ecole National Superieure d'Electricité et de Mécanique (ENSEM-INPL), France in 2007, and is currently pursuing the Ph.D. degree at the Laboratoire de Génie Electrique de Paris LGEP, CNRS UMR8507, SUPELEC, Université Paris Sud 11, Université Pierre Marie Curie, Paris, France. His current research interests include power electronics, and electrical devices (FC, batteries and supercapacitor).

Olivier Bethoux (M'09) was born in Lyon, France, in 1967. He received the M.Sc. degree from Ecole Centrale de Lille in 1990. From 1992 to 1997, he worked as a Research Engineer in the Alcatel Alsthom Research Center (France), on power converters and electrical drives. A successful candidate of Agrégation de Génie Electrique (1997), he joined the Ecole Nationale Supérieure d'Electronique et de ses Applications (ENSEA) as Associate Professor of Electrical Engineering, in 1999. In October 2005, he received a Ph.D. degree in Electrical and Computer Engineering, from the University of Cergy-Pontoise. In September 2006, he joined the Laboratoire de Génie Électrique de Paris and the IUT of Cachan, University of Paris Sud 11 as an Associate Professor of Electrical Engineering.
His main research interests and experience include analysis, design, and control of electric machines, variable speed drives for traction and propulsion applications, and fault diagnosis of electric drives. His current area of research includes advanced control techniques and energy management with new power sources like fuel cell and photovoltaic cells.

Ghislain Remy (M'06) was born in Epinal, France, in 1977. He received the teaching degree "Aggregation" from the Ecole Normale Supérieure de Cachan, France in 2001, and the Ph.D. degree from the Ecole Nationale Supérieure d'Arts et Métiers (ENSAM) of Lille, France in 2007. Since 2008, he has been an assistant professor at the Institut Universitaire de Technologie of Cachan (Université Paris-Sud) and with the Laboratoire de Génie Electrique de Paris (LGEP)/Sud de Paris Energie Electrique, CNRS UMR8507, École Supérieure d'Électricité, Université Paris VI et XI, Gif-sur-Yvette, France. His current research interests include design and control of electromechanical systems with multi-domain and multi-level approaches.

Claude Marchand (M'07) has received the degree from the Ecole Normale Supérieure de Cachan, Cachan, France, and the Ph.D. degree from the Université Paris XI, Paris, France, in 1991. Since 1988, he has been with the Laboratoire de Génie Electrique de Paris (LGEP)/Sud de Paris Energie Electrique, CNRS UMR8507, École Supérieure d'Électricité, Université Paris VI et XI, Gif-sur-Yvette, France. From 1994 to 2000, he was an Assistant Professor at the Institut Universitaire de Technologie of Cachan (Université Paris-Sud). Since 2000, he has been a Professor at the Université Paris-Sud. He is the Head of the LGEP research team "Design, Control, and Diagnosis" on electromagnetic systems. His research interests are in eddy current nondestructive testing and in design and control of electrical actuator.

Eric Berthelot was born in Puiseaux, France, in 1957. Since 1991, he has been an Engineer R&D and has joined the MOCOSEM department of the Laboratoire de Génie Electrique de Paris (LGEP). He has been responsible for the design of drive control systems and power supply converters. Currently, he has been responsible for the design and for the technology improvement of the magnetostrictive platform, the electro-magnetic actuators platform, the non destructive testing platform, and the hydrogen fuel cells platform.